

# Photo- and electrical-responsive liquid crystal smart dimmer for augmented reality displays

JAVED ROUF TALUKDER,<sup>1,2</sup> HUNG-YUAN LIN,<sup>1,2</sup> AND SHIN-TSON WU<sup>1,\*</sup>

<sup>1</sup>CREOL, The College of Optics and Photonics, University of Central Florida, Orlando, FL 32816, USA

<sup>2</sup>These authors contributed equally to this work

\* [swu@creol.ucf.edu](mailto:swu@creol.ucf.edu)

**Abstract:** A dual-stimuli polarizer-free dye-doped liquid crystal (LC) dimmer is demonstrated. The LC composition consists of photo-stable chiral agent, photosensitive azobenzene, and dichroic dye in a nematic host with positive dielectric anisotropy. Upon UV exposure, the LC directors and dye molecules turn from initially vertical alignment (high transmittance state) to twisted fingerprint structure (low transmittance state). The reversal process is accelerated by combining a longitudinal electric field to unwind the LC directors from twisted fingerprint to homeotropic state, and a red light to transform the *cis* azobenzene back to *trans*. This device can be used as a smart dimmer to enhance the ambient contrast ratio for augmented reality displays.

© 2019 Optical Society of America under the terms of the [OSA Open Access Publishing Agreement](#)

## 1. Introduction

See-through augmented reality (AR) displays, such as Google Glass, HoloLens, and Magic Leap One, are emerging due to their useful applications in education, engineering design, medical, retail, transportation, automotive, aerospace, gaming, and entertainment, just to name a few [1–7]. In such an AR system, the computer-generated images are projected to superimpose with the environment [8,9]. As the ambient brightness increases, the image contrast ratio decreases gradually [10]. To enhance ambient contrast ratio, we could either boost the display luminance or dim the incident background light through a built-in sensor. The former is called adaptive brightness control, while the latter is called smart dimmer. A smart dimmer placed in front of the AR display helps to control the incident background light, which in turn improves the ambient contrast ratio. Recently, several types of smart dimmers have been developed, such as organic and inorganic electrochromic devices [11–16], nanoparticle devices [17,18], and guest-host liquid crystal (LC) devices [8,10,19–26]. Each approach has its own pros and cons. Among them, dichroic dye (guest) doped LC (host) device is a potential candidate for smart dimmer due to its wide view, low cost, and polarizer-free characteristics [22,23]. In this device, a few percent (2-3%) of dichroic dye is doped into a nematic LC host. The electric field-induced LC director reorientation changes the absorption of dichroic dyes, which in turn alters the transmittance of the incident background light. When the polarization of the incident light is parallel to the principal axis of dichroic dyes, the absorption is strong, resulting in a lower transmittance. On the other hand, when the incident polarization is perpendicular to the dye's principal axis, the absorption is weak and the transmittance is high.

Two types of polarization-independent guest-host systems have been developed, depending on the driving methods: one is by voltage, and another is by light. Most of above-mentioned guest-host devices belong to the former. Recently, photo-responsive dye-doped LC device has been demonstrated, which is operated by light instead of voltage [24–28]. In such a device, transmittance changes from high to low by exposing a UV (or blue) light, while the reversal process is carried out by a red light. However, the response time is relatively slow (~42s), which limits its practical applications.

In this paper, we report a dual-stimuli dye-doped LC smart dimmer with a much faster response time. To achieve dual-stimuli responses, we dope some photo-stable chiral agent, photosensitive azobenzene, and dichroic dye into a nematic LC host with positive dielectric anisotropy ( $\Delta\epsilon > 0$ ). Upon UV light exposure, our device turns from initially vertical alignment (high transmittance state) to twisted fingerprint structure (dark state). The reversal process is accelerated by combining electric field (to unwind the fingerprint to homeotropic alignment) and red light (to transform azobenzene from *cis* to *trans*) because the LC host has a positive  $\Delta\epsilon$ . Such an electric-field-assisted reversal time can be reduced from  $\sim 10$  seconds to a few milliseconds, depending on the applied voltage.

## 2. Experiment

Our liquid crystal mixture consists of four components: 1-4 wt.% left-handed photo-stable chiral agent (Merck S-811), 0.3-1.3 wt.% right-handed photo-responsive chiral azobenzene compound (PSC-01) [28,29], 2 wt.% black dichroic dye (Mitsui S428), and an LC host ZLI-2976 ( $\Delta\epsilon = 11$  at  $f = 1$  kHz, clearing temperature  $T_c = 101.7^\circ\text{C}$  and birefringence  $\Delta n = 0.12$  at  $\lambda = 589$  nm). The mixture was stirred on a heating stage for several minutes to dissolve completely. Afterward, the mixture was injected to a  $9\text{-}\mu\text{m}$  homeotropic cell where the LC directors were aligned perpendicular to the glass substrates. Commercial light sources, AMSCOPE UV LED lamp (365nm), blue (450nm) and red light (633nm) sources were used to irradiate the sample. Deuterium halogen light source (DH-2000), He-Ne laser beam (633nm) and HR4000CG-UV-NIR spectrometer from Ocean Optics were used to measure the spectrum and response time at different state. We used Olympus BX51 polarizing optical microscope to take the images of the sample.

## 3. Operation principles

A smart dimmer should be polarization independent because the ambient light is unpolarized. For this purpose, we doped dichroic dyes to a helical LC structure. Dichroic dyes are low molecular weight with elongated dimension. They preferentially absorb the light polarized along the longer axis and transmit the other. However, due to limited dichroic ratio ( $< 15:1$ ), the absorption will not be perfect. When the LC directors and dichroic dyes form cholesteric structure, the absorption is insensitive to polarization. Cholesteric structure are typically prepared by adding a chiral compound to the LC host to induce helical structure. In our device, we mixed a photo-stable chiral agent (S-811) and a photosensitive azobenzene dye (PSC-01) to the dye-doped LC mixture to induce chirality. Helical twist power (HTP) is used to define the chirality, and the net HTP of our mixture depends on the competition between the left-handed chiral agent (S-811, negative HTP) and right-handed azobenzene dyes (PSC-01, positive HTP). However, the HTP of right-handed azobenzene dyes changes upon *trans-cis* isomerization [30,31]. Typically, azobenzene dyes stay in rod shape *trans*-state in the absence of UV-blue light [32,33]. It has a broad absorption spectrum near UV region and the exposure to UV light changes the molecular conformation. Hence, the *trans*-azobenzene transforms into the *cis*-state; the latter has a smaller HTP than the former.

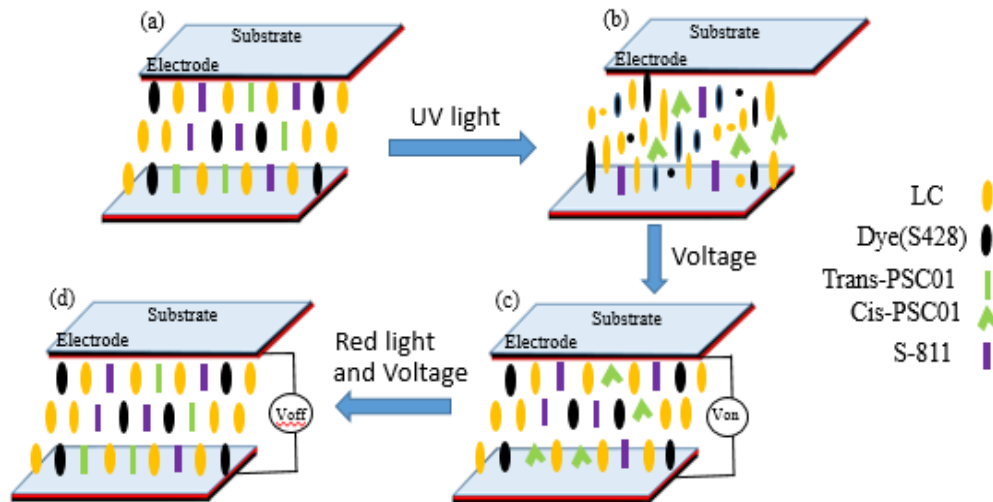


Fig. 1. Operation mechanisms of the proposed device: (a) Initial state, (b) after UV exposure, (c) with a voltage, and (d) removing the voltage and red light.

Figure 1 depicts the operation mechanisms of our device. Initially, the concentrations of S-811 and PSC-01 are carefully chosen so that the positive HTP of PSC-01 cancels out the negative HTP of S-811, i.e. the net chirality is too weak to induce cholesteric helical structure. Because the mixture is confined in a cell with sufficiently strong homeotropic anchoring, the LC directors and dichroic dyes will be aligned in vertical direction, as Fig. 1(a) shows. In this unwound state, the light absorption is minimum and the device is in the transparent state.

The threshold pitch value to form helical structure is governed by  $P_{th} = 2dK_{22}/K_{33}$ , where  $d$  is the cell gap, and  $K_{22}$  and  $K_{33}$  are the twist and bend elastic constants, respectively [34]. In an LC cell, when the net pitch value is smaller than the threshold pitch, twisted nematic structure occurs because the chiral torque is strong enough in comparison with the elastic torque. When the LC cell is exposed to UV-blue light, the *trans-cis* isomerization of azobenzene dye takes place and its positive HTP decreases while the negative HTP of photo-stable chiral agent remains unchanged. As a result, the net absolute HTP value of the mixture increases. When the pitch value is smaller than the threshold pitch, as shown in Fig. 1(b), phase transition from homeotropic texture to twisted cholesteric structure occurs. Under such an LC director configuration, the absorption of dichroic dyes is insensitive to the incident light polarization, and the device turns into dark state. A typical contrast ratio of guest-host displays is about 3-5:1. Contrast ratio can be further improved by using a better dye with larger dichroic ratio, or increasing the dye's concentration or LC layer thickness, but the last two approaches would decrease the transmittance. To change from dark to bright state, we can illuminate the device with a red light or apply a voltage. Upon red light exposure, the *cis*-azobenzene dyes are transformed back to *trans*-state, and therefore the net HTP decreases. When the net HTP is zero or weaker than the homeotropic anchoring, the pitch value exceeds the threshold value so that the helix is suppressed and the twisted fingerprint-to-homeotropic phase transition takes place. At this state, the device becomes transparent again due to minimum absorption. However, this reversal process takes around 10-20 seconds, depending on the red light intensity.

In order to accelerate the transition from dark to transparent state, we can also apply a voltage. Because our employed nematic host has a *positive* dielectric anisotropy, the LC directors and dichroic dyes will be unwound from fingerprint to homeotropic state by the electric field. When a longitudinal electric field is applied at *cis*-state where the device

appears dark, as the electric torque exceeds the chiral torque, the LC directors and dyes will be reoriented back to their initial homeotropic state although the azobenzene molecules remain in *cis*-state [Fig. 1(c)]. Under such condition, as will be shown in next section, the transmittance remains the same as that of Fig. 1(a). However, if the voltage is removed, the device will return to dark state quickly [Fig. 1(b)]. If we keep irradiating red light to the device for about 10-15 seconds (no matter the voltage is on or off), the *cis*-azobenzene will be converted back to *trans*-state and the chiral torque is weaker than the surface anchoring. As a result, the device will stay at transparent state even if we turn-off the voltage. As shown in Fig. 1(d), both LC directors and dyes are in vertical alignment and azobenzene is in *trans*-state, which is the same as Fig. 1(a).

#### 4. Results and discussion

We first measured the dichroic ratio of Mitsui dye S428 in the LC host ZLI-2976. To do so, we prepared 3 homogeneous LC cells with 9- $\mu\text{m}$  gap and 1%, 2%, and 4% dye concentrations, and measured their transmittance  $T = \exp(-ad)$ , where  $ad$  represents the absorbance. Figure 2 shows the measured absorbance in two orthogonal polarizations. When the incident polarization is parallel to the long axis of dye molecules, the absorption is high (red line). However, when the polarization of incident light is perpendicular to the long axis of dye molecules, the absorption is decreased (black line). From the slopes of these two straight lines shown in Fig. 2, we obtain the dichroic ratio of Mitsui S428 is 11.6 in the ZLI-2976 LC host.

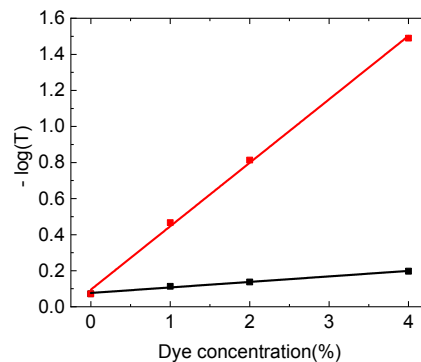


Fig. 2. Measured absorption anisotropy of Mitsui S428 dye at  $\lambda = 633$  nm. Red and black dots correspond to the polarization parallel and perpendicular to the LC directors. LC host ZLI-2976.

Figure 3 shows the measured transmission spectrum of our guest-host device from 400 nm to 700 nm at the room temperature (22°C). The results shown in Fig. 3 are obtained from the sample containing 4wt% chiral agent and 0.7wt% azobenzene dye. At initial state, the transmittance is relatively high (60-70%) in the visible region due to low absorption loss. Limited dichroic ratio, order parameter, and surface reflection also contribute to the rest of the loss. When the sample is irradiated with a UV light ( $\lambda \approx 365$  nm) at 10 mW/cm<sup>2</sup> intensity, its transmittance decreases in the visible region, as the red line in Fig. 3 shows. For example, at 550 nm, the transmittance drops from ~70% to ~23%. After UV exposure, the LC directors and dichroic dyes turn into twisted fingerprint state. In this state, dichroic dyes strongly absorb the incident light and the device turns to dark state including ~5% scattering. When the UV light is removed, the device stays at fingerprint state. The twisted fingerprint state is very stable and can last for more than 10 hours.

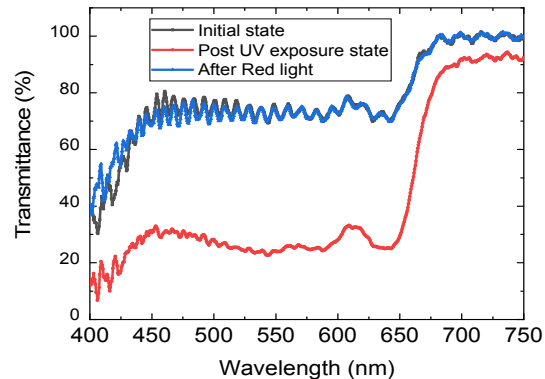


Fig. 3. Measured transmission spectra at initial state, post UV exposure, and after red light exposure.

The reversal process from dark to bright state was carried out by exposing the sample with a red light (633nm) at  $5.5 \text{ mW/cm}^2$  intensity (blue line in Fig. 3). Besides red light, the reversal process can also be carried out by voltage. Figure 4 shows the measured transmittance change after applying different voltages at the post UV exposure state. As the voltage increases, the LC directors and dichroic dyes start to unwind but the transmittance decreases initially due to light scattering. Above 6V, transmittance starts to increase because of the reduced absorption and scattering. At  $\sim 10\text{V}$ , the LC directors and dyes are unwound completely and they turn into homeotropic state whereas azobenzene remains in the *cis*-state. Therefore, the device returns back to transparent state. Please note the electric field alone cannot transform the *cis*-azobenzene back to *trans*-state; additional red (or green) light exposure is required.

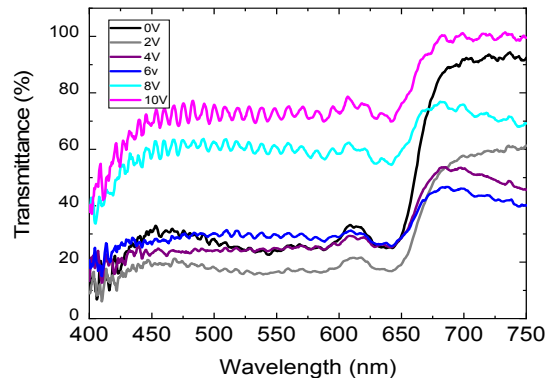


Fig. 4. Measured transmission spectra of post UV exposure state under different voltages.

Figure 5 shows the images behind our dimmer at different states. The photos were taken under the lab yellow lighting environment. Figure 5(a) shows the transparent image at initial state where the sample is not exposed to UV light. From this image we can easily recognize the colored word “LCD”. Figure 5(b) shows the image at post UV exposure state. The image becomes dark as transmittance decreases due to *trans-cis* isomerization. Contrast ratio can be improved by increasing the dichroic dye concentration or using a thicker cell gap, but the trade-off is decreased transmittance. We applied 10V in the center area (with indium tin oxide (ITO) electrodes) at post UV exposure state and the image in this state is shown in Fig. 5(c). The LCs and dyes in the electrode area are reversed back to the initial vertical state due to strong electric field, so that the image “LCD” becomes transparent again. However, the

azobenzene remains in the cis-state (Fig. 1(c)). To convert the cis back to trans, we exposed the sample with a red light ( $\lambda = 633 \text{ nm}$  at intensity =  $5.5 \text{ mW/cm}^2$ ) for  $\sim 20$  seconds. This process is independent of whether the voltage is on or off. Figure 5(d) shows the transparent image, which is the same as Fig. 5(a).

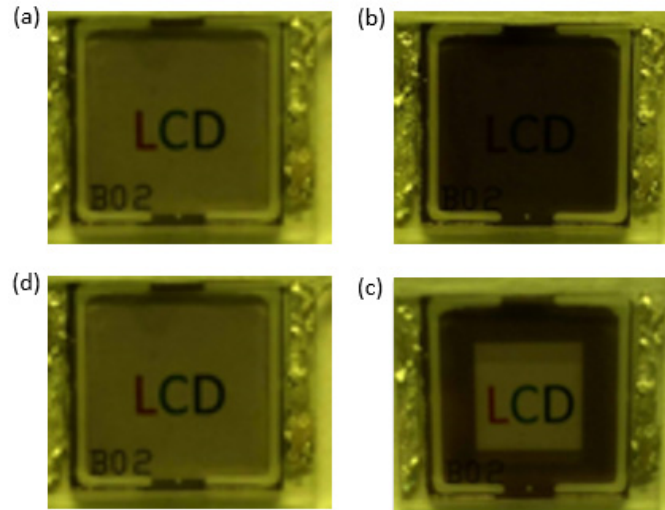


Fig. 5. See-through image behind the dimmer: (a) Initial state, (b) Post UV exposure state, (c) After applying 10V at post UV exposure state (the dark area has no electrode), and (d) After red light irradiation for 15 s at post UV exposure state.

We also measured the response time of our device from bright (Fig. 5(a)) to dark state (Fig. 5(b)) upon UV exposure. Figure 6 shows the measured transmittance (at  $\lambda = 633 \text{ nm}$ ) versus UV exposure time. The intensity of UV light was measured as  $10 \text{ mW/cm}^2$ . From Fig. 6, the response time (defined as transmittance changes from 90% to 10%) is 1.3 second. This response time could be further decreased by increasing the UV intensity [24] or using a faster azobenzene material [35]. It should be mentioned that this device stayed at dark state several hours after the UV light was turned off.

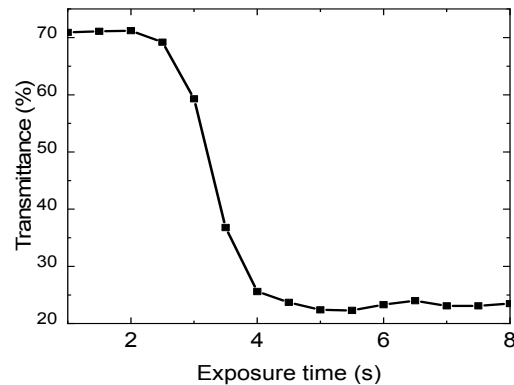


Fig. 6. Measured transmittance change at  $\lambda = 633 \text{ nm}$  of our device upon UV exposure ( $10 \text{ mW/cm}^2$ ).

At the post-UV exposure state, we applied 10V to the LC sample for 500 ms and recorded the reversal time from dark state to bright state. Results are shown in Fig. 7. From Fig. 7, the reversal time from dark to bright is about 202 ms. If we increase the voltage to 50V, then the reversal time is reduced to  $\sim 8$  ms. This reversal time is much faster than that of photo-driven

device reported earlier [24]. However, when we turned off the voltage the device returns back to dark state within 36.7 ms, as shown in Fig. 7. This is because the *cis*-azobenzene molecules bring the neighboring LCs and dyes back to the twisted fingerprint state, which is a stable state (Fig. 5(b)). On the other hand, the voltage-on state (Fig. 5(c)) is not a stable state, although its transmittance is the same as that of original state. To work as a dimmer, we can operate the device between these two states [Fig. 5(b) and 5(c), corresponding to Fig. 1(b) and 1(c)] because of its fast response time.

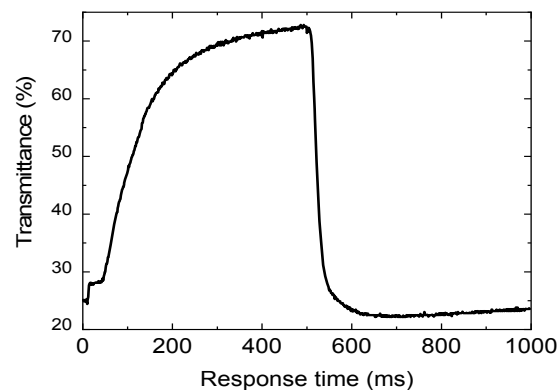


Fig. 7. Measured transmittance (at 633 nm) vs. response time at post UV exposure state after applying 10 V for 500 ms.

In order to return to the original stable state, we need to expose the sample with a red light. In experiment, we used a HeNe laser beam with  $\lambda = 633$  nm and intensity =  $5.5$  mW/cm<sup>2</sup>. Figure 8 shows the measured results. Due to red light irradiation, reversal *cis-trans* isomerization takes place and the HTP of azobenzene dye is slowly decreasing. After ~15-20 seconds (Fig. 8), the HTP of left-handed S-811 and right-handed PSC-01 cancels out each other and the device stays transparent even if we remove the red light. Some groups are exploring the possibility of electro-isomerization of azobenzene materials. If successful, then we can eliminate the step of red light exposure [36,37].

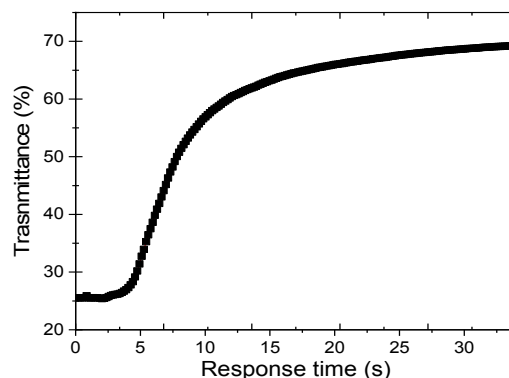


Fig. 8. Measured time-dependent transmittance of the LC sample from the post exposure state after HeNe laser beam exposure at intensity =  $5.5$  mW/cm<sup>2</sup>.

Next, we investigate how the concentration of left-handed chiral agent S-811 affects the performance of our device. We prepared four samples by varying the S-811 concentration from 1 wt.% to 5 wt.%, while keeping other material's concentration unchanged (0.7% PSC and 2% S-428) and inspected the samples under a polarizing optical microscope between

crossed polarizers. Figure 9(a)-(d) shows the microscopic image at initial state and post UV exposure state for the 1%, 3% and 4% of S-811 samples. As shown in Fig. 9(a), at initial state with 1%, 3%, and 4% concentrations the microscope image looks black because the LC directors and dyes are aligned perpendicular to the substrates. However, at the post UV exposure state (Fig. 9(b)-(d)), the fingerprint textures appear. As the concentration of S-811 increases, the pitch of fingerprint state decreases and well-defined fingerprint texture forms which reduces light scattering.

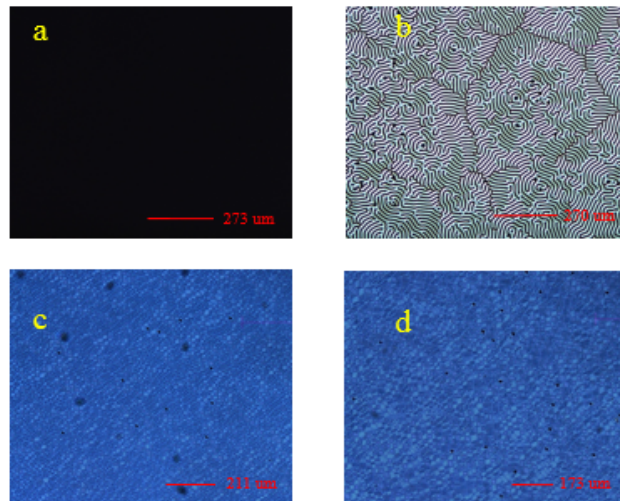


Fig. 9. Microscope images of four samples: (a) Initial state (1%-4% S-811), (b) 1% S-811, (c) 3% S-811, and (d) 4% S-811 at post UV exposure state.

Finally, we prepared four samples by varying the concentration of azobenzene from 0.3% to 1.6%, while keeping 4% S-811. Figure 10 shows the measured results of transmittance versus azobenzene concentration in the post UV exposure state and after voltage. From Fig. 10, we do not observe any noticeable difference in transmittance in both bright and dark states. It is apparent that at initial state, the HTP of azobenzene within this concentration range still cancels out the HTP of the 4% S-811. However, if azobenzene concentration is lower than 0.3% (with 4% S-811), this device does not work as a dimmer based on our proposed mechanisms.

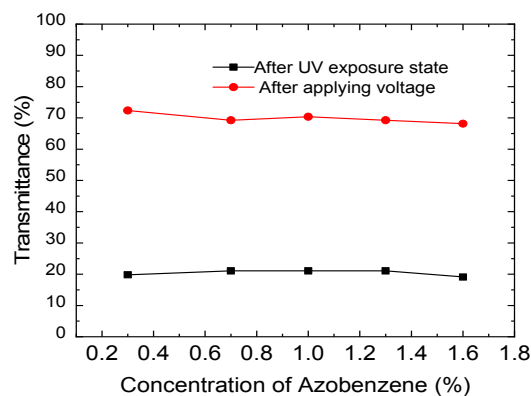


Fig. 10. Measured transmittance at different azobenzene concentrations.  $\lambda = 550$  nm.

Lower birefringence liquid crystal helps to suppress the polarization rotation effect of the incident light. Therefore, we also used a lower  $\Delta n$  mixture (ZLI 1800-100,  $\Delta n = 0.07$ , nematic range from  $-20^{\circ}\text{C}$  to  $61^{\circ}\text{C}$ ) as host and injected the mixture into a  $9\text{-}\mu\text{m}$  homeotropic cell. Results (Fig. 11) are very similar to those of ZLI-2976 (Fig. 3) as transmittance of our device mostly depends on the absorption properties of the employed dichroic dye.

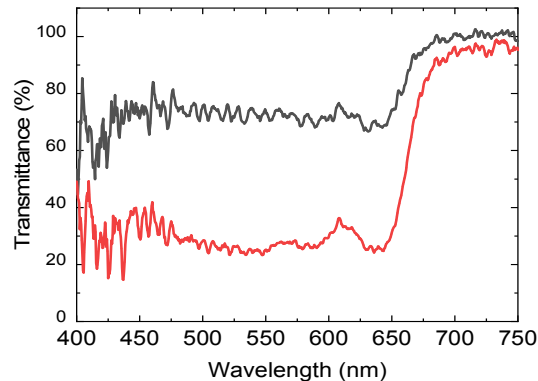


Fig. 11. Measured transmission spectra at initial state (black line) and post UV exposure state (red line) using a low birefringence LC host, ZLI 1800-100.

## 5. Conclusion

We have demonstrated a polarizer-free dual-responsive LC dimmer consisting of chiral compound, dichroic dye, azobenzene, and LC host. Using photo-responsivity of azobenzene dye and absorption properties of dichroic dyes, photo-switching from bright state to dark state is achieved by irradiating UV light. Reversal process from dark to bright state of our device can be carried out by applying a voltage or exposing a red light, or combined together, which offers a significantly faster response time than the previously reported photo-responsive device. Considering its low manufacturing cost and large fabrication tolerance, our photo-responsive device can be used as a light dimmer for augmented reality displays.

## Funding

Air Force Office of Scientific Research (AFOSR) (FA9550-14-1-0279).

## Acknowledgments

The authors would like to thank Prof. Huai Yang for providing the chiral azobenzene material, and Yun-Han Lee, Ran Chen, and Guanjun Tan for helpful technical discussion.

## Disclosures

The authors declare that there are no conflicts of interest related to this article.

## References

1. J. P. Rolland and H. Fuchs, "Optical versus video see-through head-mounted displays in medical visualization," *Presence-Teleop. Virt.* **9**(12), 287–309 (2000).
2. J. Wang, H. Suenaga, K. Hoshi, L. Yang, E. Kobayashi, I. Sakuma, and H. Liao, "Augmented reality navigation with automatic marker-free image registration using 3-D image overlay for dental surgery," *IEEE Trans. Biomed. Eng.* **61**(4), 1295–1304 (2014).
3. T. Sielhorst, M. Feuerstein, and N. Navab, "Advanced medical displays: a literature review of augmented reality," *J. Disp. Technol.* **4**(4), 451–467 (2008).
4. X. Hu and H. Hua, "High-resolution optical see-through multi-focal-plane head-mounted display using freeform optics," *Opt. Express* **22**(11), 13896–13903 (2014).
5. P. E. Kourouthanassis, C. Boletis, and G. Lekakos, "Demystifying the design of mobile augmented reality applications," *Multimedia Tools Appl.* **74**(3), 1045–1066 (2015).

6. X. Wang and P. S. Dunston, "Comparative effectiveness of mixed reality-based virtual environments in collaborative design," *IEEE Trans. Syst., Man, Cybern. Syst. Part C* **41**(3), 284–296 (2011).
7. H. Regenbrecht, G. Barattoff, and W. Wilke, "Augmented reality projects in the automotive and aerospace industries," *IEEE Comput. Graph. Appl.* **25**(6), 48–56 (2005).
8. R. Zhu, H. Chen, T. Kosa, P. Coutino, G. Tan, and S. T. Wu, "High-ambient-contrast augmented reality with a tunable transmittance liquid crystal film and a functional reflective polarizer," *J. Soc. Inf. Disp.* **24**(4), 229–233 (2016).
9. S. Lee, X. Hu, and H. Hua, "Effects of optical combiner and IPD change for convergence on near-field depth perception in an optical see-through HMD," *IEEE Trans. Vis. Comput. Graph.* **22**(5), 1540–1554 (2016).
10. R. Zhu, G. Tan, J. Yuan, and S. T. Wu, "Functional reflective polarizer for augmented reality and color vision deficiency," *Opt. Express* **24**(5), 5431–5441 (2016).
11. R. Chen, Y. H. Lee, T. Zhan, K. Yin, Z. An, and S. T. Wu, "Multi-stimuli-responsive self-organized liquid crystal Bragg gratings," *Adv. Opt. Mater.* **7**(9), 1900101 (2019).
12. E. L. Runnerstrom, A. Llordés, S. D. Lounis, and D. J. Milliron, "Nanostructured electrochromic smart windows: traditional materials and NIR-selective plasmonic nanocrystals," *Chem. Commun. (Camb.)* **50**(73), 10555–10572 (2014).
13. A. Tsuboi, K. Nakamura, and N. Kobayashi, "Multicolor electrochromism showing three primary color states (cyan–magenta–yellow) based on size- and shape-controlled silver nanoparticles," *Chem. Mater.* **26**(22), 6477–6485 (2014).
14. Y.-M. Zhang, X. Wang, W. Zhang, W. Li, X. Fang, B. Yang, M. Li, and S. X.-A. Zhang, "A single-molecule multicolor electrochromic device generated through medium engineering," *Light Sci. Appl.* **4**(2), e249 (2015).
15. J. A. Kerszulis, C. M. Amb, A. L. Dyer, and J. R. Reynolds, "Follow the yellow brick road: structural optimization of vibrant yellow-to-transmissive electrochromic conjugated polymers," *Macromolecules* **47**(16), 5462–5469 (2014).
16. S. V. Vasilyeva, P. M. Beaujuge, S. Wang, J. E. Babiarz, V. W. Ballarotto, and J. R. Reynolds, "Material strategies for black-to-transmissive window-type polymer electrochromic devices," *ACS Appl. Mater. Interfaces* **3**(4), 1022–1032 (2011).
17. W. Wen, C. Weisbuch, D. Phuong, G. Lu, W. Ge, C. T. Chan, and P. Sheng, "Neutral nanoparticle-based display," *Nanotechnology* **16**(4), 598–601 (2005).
18. A. Ghosh, B. Norton, and A. Duffy, "Measured overall heat transfer coefficient of a suspended particle device switchable glazing," *Appl. Energy* **159**, 362–369 (2015).
19. J. Heo, J.-W. Huh, and T.-H. Yoon, "Fast-switching initially-transparent liquid crystal light shutter with crossed patterned electrodes," *AIP Adv.* **5**(4), 047118 (2015).
20. Y.-H. Lin, J.-M. Yang, Y.-R. Lin, S.-C. Jeng, and C.-C. Liao, "A polarizer-free flexible and reflective electrooptical switch using dye-doped liquid crystal gels," *Opt. Express* **16**(3), 1777–1785 (2008).
21. G. H. Lee, K. Y. Hwang, J. E. Jang, Y. W. Jin, S. Y. Lee, and J. E. Jung, "Characteristics of color optical shutter with dye-doped polymer network liquid crystal," *Opt. Lett.* **36**(5), 754–756 (2011).
22. C.-T. Wang and T.-H. Lin, "Bistable reflective polarizer-free optical switch based on dye-doped cholesteric liquid crystal [Invited]," *Opt. Mater. Express* **1**(8), 1457–1462 (2011).
23. Y. H. Lin, H. W. Ren, and S. T. Wu, "High contrast polymer-dispersed liquid crystal in a 90° twisted cell," *Appl. Phys. Lett.* **84**(20), 4083–4085 (2004).
24. J. R. Talukder, Y. H. Lee, and S.-T. Wu, "Photo-responsive dye-doped liquid crystals for smart windows," *Opt. Express* **27**(4), 4480–4487 (2019).
25. D. K. Yang, J. W. Doane, Z. Yaniv, and J. Glasser, "Cholesteric reflective display: drive scheme and contrast," *Appl. Phys. Lett.* **64**(15), 1905–1907 (1994).
26. A. Bobrovsky, N. Boiko, V. Shibaev, and J. Wendorff, "Photoinduced textural and optical changes in a cholesteric copolymer with azobenzene-containing side groups," *Liq. Cryst.* **31**(3), 351–359 (2004).
27. C. T. Wang, Y. C. Wu, and T. H. Lin, "Photo-controllable tristable optical switch based on dye-doped liquid crystal," *Dyes Pigments* **103**, 21–24 (2014).
28. Y. H. Lee, L. Wang, H. Yang, and S.-T. Wu, "Photo-induced handedness inversion with opposite-handed cholesteric liquid crystal," *Opt. Express* **23**(17), 22658–22666 (2015).
29. Q. Li, L. Green, N. Venkataraman, I. Shiyankovskaya, A. Khan, A. Urbas, and J. W. Doane, "Reversible photoswitchable axially chiral dopants with high helical twisting power," *J. Am. Chem. Soc.* **129**(43), 12908–12909 (2007).
30. S. Kurihara, S. Nomiyama, and T. Nonaka, "Photochemical control of the macrostructure of cholesteric liquid crystals by means of photoisomerization of chiral azobenzene molecules," *Chem. Mater.* **13**(6), 1992–1997 (2001).
31. J. Bin and W. S. Oates, "A unified material description for light induced deformation in azobenzene polymers," *Sci. Rep.* **5**(1), 14654 (2015).
32. S. Kundu and S.-W. Kang, "Photo-stimulated phase and anchoring transitions of chiral azo-dye doped nematic liquid crystals," *Opt. Express* **21**(25), 31324–31329 (2013).
33. M. Mathews, R. S. Zola, S. Hurley, D.-K. Yang, T. J. White, T. J. Bunning, and Q. Li, "Light-driven reversible handedness inversion in self-organized helical superstructures," *J. Am. Chem. Soc.* **132**(51), 18361–18366 (2010).

34. B. Y. Zeldovich and N. V. Tabiryan, "Equilibrium structure of a cholesteric with homeotropic orientation on the walls," *Sov. Phys. JETP* **56**, 563–566 (1982).
35. U. Hrozhyk, S. Serak, N. Tabiryan, D. Steeves, L. Hoke, and B. Kimball, "Azobenzene liquid crystals for fast reversible optical switching and enhanced sensitivity for visible wavelengths", *Liquid Crystals XIII*, ed. by I.-C. Khoo, *Proc. SPIE*, **7414**, 74140L (2009).
36. Y.-C. Liu, K.-T. Cheng, H.-F. Chen, and A. Y.-G. Fuh, "Photo- and electro-isomerization of azobenzenes based on polymer-dispersed liquid crystals doped with azobenzenes and their applications," *Opt. Express* **22**(4), 4404–4411 (2014).
37. Z. F. Liu, K. Hashimoto, and A. Fujishima, "Photoelectrochemical information storage using an azobenzene derivative," *Nature* **347**(6294), 658–660 (1990).